Model for electron detachment from negative ions by ultrashort half-cycle electric-field pulses

T. P. Grozdanov* and J. Jaćimović
Institute of Physics, Pregrevica 118, 11080 Belgrade, Serbia
(Received 30 October 2008; published 15 January 2009)

We study a model for electron detachment from negative ions by ultrashort unipolar electric pulses. The electron-atom interaction is described by the zero-range potential and the temporal dependence of the electric field is approximated by the Dirac δ functions. The case of a single pulse can be treated semianalytically and explicit expressions are obtained for momentum and energy distributions of detached electrons as well as for the total detachment probability. The determination of angular distribution involves numerical evaluation of a one-dimensional integral. The case of two alternating electric pulses requires numerical evaluation of more complicated integrals but leads to interesting effects caused by the quantum interference of the electronic wave packets produced during the interactions with the first and the second pulses. The differential and integral detachment probabilities are calculated and discussed for a variety of pulse strengths and time delays between the pulses.

DOI: 10.1103/PhysRevA.79.013413 PACS number(s): 32.80.Gc, 42.50.Hz

I. INTRODUCTION

The description of the motion of an electron in the zero range potential (ZRP) has served as a useful model for studies of many processes involving negative ions in interactions with external fields or collisions with other atomic particles [1]. In particular, the model has been widely used in describing interaction of negative ions with strong monochromatic laser fields (see the review article [2], and references therein).

In recent years, great experimental advances have been achieved in developing short pulses of uv to xuv light of sub-femtosecond duration (see, e.g., the review [3]), aimed for the studies of the ultrafast phenomena in atomic and molecular physics. For example, isolated, approximately single-cycle attosecond pulses with a duration of about 130 as and a photon energy of about 36 eV have been realized [4]. In the context of theoretical description of electron detachment by few-cycle laser pulses, the ZRP model was first used within the Keldysh-type strong-field approximation (SFA) applied to H^- ion [5]. The validity of this approach is restricted to situations when the pulse duration is much longer than the characteristic orbiting time of the loosely bound electron and the depletion of the initial state is small. More recently, the ZRP model was used to study the dependence of the detachment probability on the duration of the few-cycle pulses, by using the first-order perturbation theory, adiabatic (tunneling) approximation, SFA and exact solution of the time-dependent Schrödinger equation [6,7].

In the present work we use the ZRP model to study in some details the detachment caused by the action of one or two alternating ultrashort unipolar electric pulses, known also as "half-cycle pulses" (HCPs). It is assumed that the duration of each of these HCPs is much smaller then the electron orbiting time in the initial state, so that the actual form of the HCP is unimportant. Each HCP is characterized by the total momentum transferred to the electron during the interaction. Previously, such sudden "kicks" of electrons by HCPs have been studied theoretically in the context of ionization of atomic Rydberg states [8–10] and more recently, in the context of the ionization from the ground state of hydrogen [11,12].

The plan of this paper is as follows. In Sec. II we consider the case of a single ultrashort half-cycle pulse interacting with a negative ion. Most of the results concerning the total and differential detachment probabilities can be obtained analytically and therefore analyzed in full details. Section III deals with the case of two alternating ultrashort pulses where the determination of detachment probabilities involves numerical evaluation of certain type of integrals. The most significant effect in this case, the quantum interference of the wave packets formed during the interaction with each of the pulses, can be fully described and analyzed by studying momentum distributions of the detached electrons. These effects are to some extent smoothed out in partially integrated energy and angular distributions. However, the remnants of the interference effects are present even in the total detachment probabilities. Some concluding remarks are given in Sec. IV. We use atomic units throughout the work except when explicitly stated.

II. SINGLE ULTRASHORT HALF-CYCLE PULSE

Within the single-active-electron approximation for a negative ion, the motion of the outer electron in the combined fields of the atom and the linearly polarized electric pulse $\mathbf{F}(t)$ is described, in the dipole approximation, by the time-dependent Schrödinger equation

$$i\frac{\partial\psi(\mathbf{r},t)}{\partial t} = [H_0 + \mathbf{F}(t)\cdot\mathbf{r}]\psi(\mathbf{r},t), \tag{1}$$

where

$$H_0 = -\tfrac{1}{2}\Delta + V(\mathbf{r}), \tag{2}$$

and the three-dimensional ZRP is defined as

*tasko@phy.bg.ac.yu

$$V(\mathbf{r}) = \frac{2\pi}{\alpha}\delta(\mathbf{r})\frac{\partial}{\partial r}r. \tag{3}$$

H_0 supports a single bound state with energy $E_b=-\alpha^2/2$ and with the corresponding normalized wave function

$$\psi_b(\mathbf{r}) = \left(\frac{\alpha}{2\pi}\right)^{1/2}\frac{e^{-\alpha r}}{r}. \tag{4}$$

The continuum (scattering) states corresponding to the asymptotic momentum $\mathbf{k}$ and outgoing (incoming) spherical waves are given by

$$\psi_{\mathbf{k}}^{\pm}(\mathbf{r}) = (2\pi)^{-3/2}\left(e^{i\mathbf{k}\cdot\mathbf{r}} - \frac{1}{\alpha \pm ik}\frac{e^{\pm ikr}}{r}\right). \tag{5}$$

The single parameter α of the ZRP is usually determined from the experimental or theoretical value of the electron affinity. For H^- we have $E_b=-0.027\,75$ and $\alpha=0.2356$.

As for the electric field, we shall assume that it is a unipolar, half-cycle pulse of arbitrary form (e.g., sine, sine-square, rectangular, etc.) with polarization along the z axis. However, the duration time of the pulse T is assumed to be much smaller than the characteristic period for Bohr transitions

$$T \ll T_c \equiv \frac{2\pi}{|\Delta E|}, \tag{6}$$

where ΔE is the energy difference between the initial and the nearest energy level. Thus, in the case of an electron in the Rydberg state with large principal quantum number n, we have $|\Delta E| \approx 1/n^3$ and $T_c \approx 2\pi n^3$, which corresponds to classical orbiting time (period) of the Rydberg electron. The ZRP has no classical analog and the notion of electron orbiting time is not applicable. Nevertheless, since there is only one bound state, $|\Delta E|=|E_b|=\alpha^2/2$ (electron affinity) and the condition (6) becomes

$$T \ll T_c = \frac{4\pi}{\alpha^2}. \tag{7}$$

In the case of H^- one has $T_c=226.39$ a.u.$=5.476$ fs, so that half-cycle pulses in the subfemtosecond region are considered.

For such ultrashort pulses one can use either the theory of sudden perturbations [13] or the Magnus expansion of the evolution operator [14,15]. The leading term for the transition amplitude is the same in both approaches and up to an unimportant phase factor is given by [8–12,16]

$$a_{fi}(\mathbf{q}) = \langle\psi_f|e^{-i\mathbf{q}\cdot\mathbf{r}}|\psi_i\rangle, \tag{8}$$

where

$$\mathbf{q} = \int_0^T \mathbf{F}(t)dt \tag{9}$$

is the momentum transferred to the electron by the electric field during the half-cycle pulse and $|\psi_i\rangle$ and $|\psi_f\rangle$ are initial and final eigenstates of H_0.

The same result for the transition amplitude, Eq. (8), is obtained if we formally replace the actual temporal form $\mathbf{F}(t)$ of the electric field by

$$\tilde{\mathbf{F}}(t) = \mathbf{q}\,\delta(t), \tag{10}$$

where $\delta(t)$ is the Dirac δ function. One should be aware of the formal character of this substitution. For example, the question whether or not the dipole approximation is applicable in our problem should be addressed to the actual physical realization of the electromagnetic pulse. Since the characteristic extension of the electronic cloud in the initial state (4) is of the order of $1/\alpha$, the condition of the applicability of the dipole approximation is $\lambda \gg 1/\alpha$, where λ is the wavelength of the carrier wave. In the case of H^-, the condition is $\lambda \gg 4.24$ a.u.$=0.225$ nm, or for the period of the carrier wave $\lambda/c \gg 0.031$ a.u.$=0.75$ as. The last condition is certainly not in contradiction with the requirement (7).

A. Total detachment probability

The probability amplitude for the electron to remain in the bound state $|\psi_b\rangle$ described by the wave function (4), after the interaction with the pulse of the form (10), can be calculated in closed form (see the Appendix):

$$a_{bb}(\mathbf{q}) = \langle\psi_b|e^{-i\mathbf{q}\cdot\mathbf{r}}|\psi_b\rangle = \frac{2\alpha}{q}\arctan\frac{q}{2\alpha}. \tag{11}$$

We note that the above, as well as all of the following results can also be obtained by using momentum representation. The calculations are in that case facilitated by the fact that the operator $\exp(-i\mathbf{q}\cdot\mathbf{r})$ is the displacement operator in momentum representation.

The probability of the electron to remain in the bound state ("survival probability") is

$$w_b = |a_{bb}(\mathbf{q})|^2 = \frac{4\alpha^2}{q^2}\arctan^2\frac{q}{2\alpha}, \tag{12}$$

and the total detachment probability is

$$w_d = 1 - w_b. \tag{13}$$

These two probabilities are shown in Fig. 1 as functions of $q'=q/\alpha$—the scaled momentum transferred to the electron. Actually, from Eqs. (1)–(5) one can easily see that our problem allows for the universal scaling, $r'=\alpha r$, $t'=\alpha^2 t$, $F'=F/\alpha^3$, $E'=E/\alpha^2$, $k'=k/\alpha$, but we shall keep the explicit dependence on α in all of our formulas.

For example, in the case of H^-, assuming a pulse of duration $T=130$ as and (for simplicity) of the rectangular form ($q=FT$), the range from $q/\alpha=0.1$ to 50, shown in Fig. 1, corresponds to the range of electric field strengths from $F=2.254\times10^7$ V/cm to 1.127×10^{10} V/cm.

B. Momentum, energy, and angular distributions of detached electrons

The transition amplitude for the electron detachment into the continuum state $|\psi_{\mathbf{k}}^-\rangle$ can also be calculated in closed form (see the Appendix),

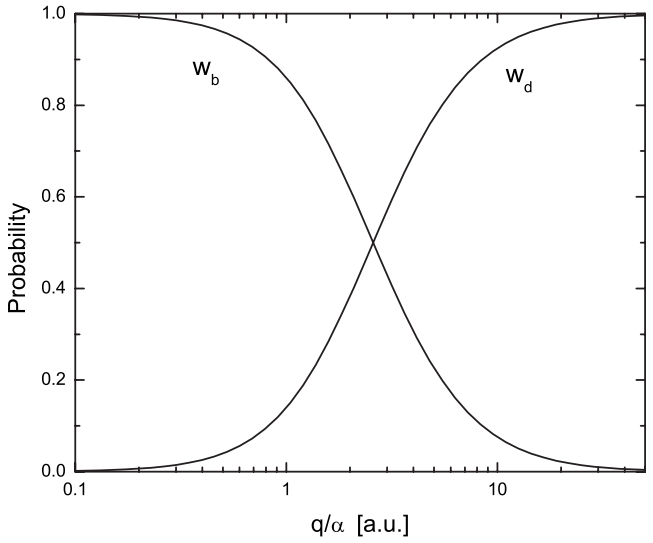

FIG. 1. Total probabilities for the electron to remain in the bound state (w_b) and to be detached ($w_d=1-w_b$) after interaction with a single pulse of the form (10) as functions of the scaled momentum transferred to the electron.

$$a_{\mathbf{k}b}(\mathbf{q}) = \langle \psi_{\mathbf{k}}^{-} | e^{-i\mathbf{q}\cdot\mathbf{r}} | \psi_b \rangle = \frac{\alpha^{1/2}}{2\pi} \times \left(\frac{2}{\alpha^2 + |\mathbf{k}+\mathbf{q}|^2} - \frac{1}{iq(\alpha+ik)} \ln \frac{\alpha - i(k-q)}{\alpha - i(k+q)} \right). \tag{14}$$

The corresponding momentum distribution (triple differential detachment probability) is given by

$$\frac{d^3 w_d}{k^2 dk \sin\theta d\theta d\phi} = |a_{\mathbf{k}b}(\mathbf{q})|^2 = \frac{\alpha}{4\pi^2} \times \left[\left(\frac{2}{\alpha^2 + k^2 + q^2 + 2kq\cos\theta} + A \right)^2 + B^2 \right], \tag{15a}$$

$$A = \frac{1}{q(\alpha^2+k^2)} \left[\frac{k}{2} \ln \frac{\alpha^2 + (k-q)^2}{\alpha^2 + (k+q)^2} + \alpha \left(\arctan \frac{k-q}{\alpha} - \arctan \frac{k+q}{\alpha} \right) \right], \tag{15b}$$

$$B = \frac{1}{q(\alpha^2+k^2)} \left[\frac{\alpha}{2} \ln \frac{\alpha^2 + (k-q)^2}{\alpha^2 + (k+q)^2} - k \left(\arctan \frac{k-q}{\alpha} - \arctan \frac{k+q}{\alpha} \right) \right]. \tag{15c}$$

The above distribution is axially symmetric (does not depend on ϕ) and instead of the spherical coordinates of the electron's momentum $\{k,\theta,\phi\}$ we can equally well use the cylindrical coordinates $\{k_\rho, k_z, \phi\}$.

The momentum distributions (15) corresponding to values of the momentum transferred to the electron $q/\alpha=0.5$, 5, and 20 are shown in Fig. 2. One can see from Fig. 2(a) that in the case $q/\alpha=0.5$ the electrons are emitted in both directions along the z axis. This is the remnant of the purely dipole distribution which is obtained from Eq. (14) in the limit $q \to 0$,

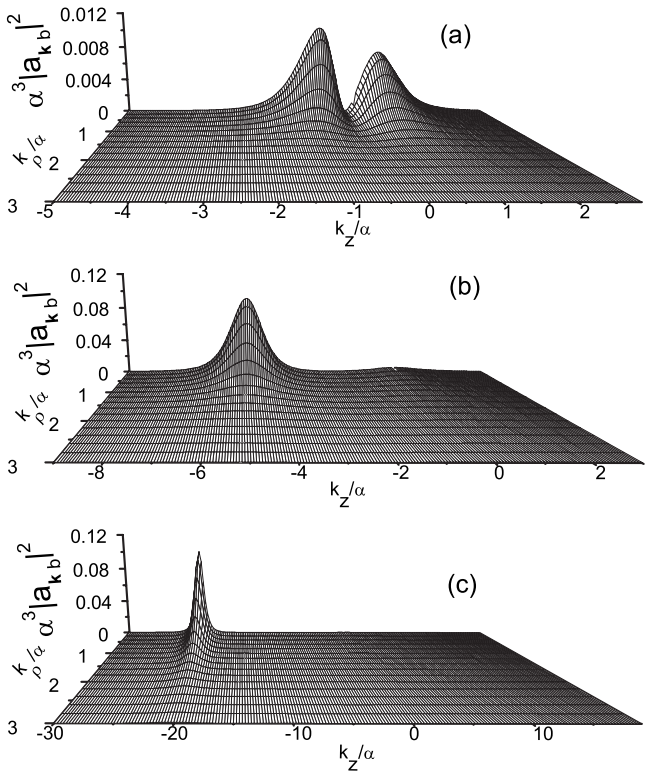

FIG. 2. Scaled momentum distributions of detached electrons for three values of the scaled momentum transferred by the pulse: (a) $q/\alpha=0.5$, (b) $q/\alpha=5$, and (c) $q/\alpha=20$. All quantities are given in a.u.

$$a^d_{\mathbf{k}b}(\mathbf{q}) = -i\mathbf{q}\cdot\langle \psi_{\mathbf{k}}^{-} | \mathbf{r} | \psi_b \rangle = -\frac{2\alpha^{1/2} qk\cos\theta}{\pi(\alpha^2+k^2)^2}. \tag{16}$$

As q/α increases [see Fig. 2(b)] a peak in the momentum distribution is beginning to build up at $k_z=-q$, while the probability for the electron emission in the positive direction of the z axis diminishes. Finally, at still larger values of the q/α, as seen from Fig. 2(c), the spectrum is dominated by the very sharp peak located at $k_z=-q$. In all cases the probability density monotonically decreases in the radial k_ρ direction.

When the momentum distribution (15a) is integrated over all angles one obtains the energy distribution ($dE=kdk$) of the detached electrons,

$$\frac{dw_d}{dE} = \frac{\alpha k}{\pi} \left(\frac{4}{(\alpha^2+k^2+q^2)^2 - 4k^2q^2} + \frac{A}{qk} \ln \frac{\alpha^2+k^2+q^2+2kq}{\alpha^2+k^2+q^2-2kq} + A^2 + B^2 \right). \tag{17}$$

The above energy distributions are shown in Fig. 3 for the values of $q/\alpha=0.1$, 0.5, 5, and 20. The peaks which show up in the cases of $q/\alpha=5$ and 20 correspond to those repre-

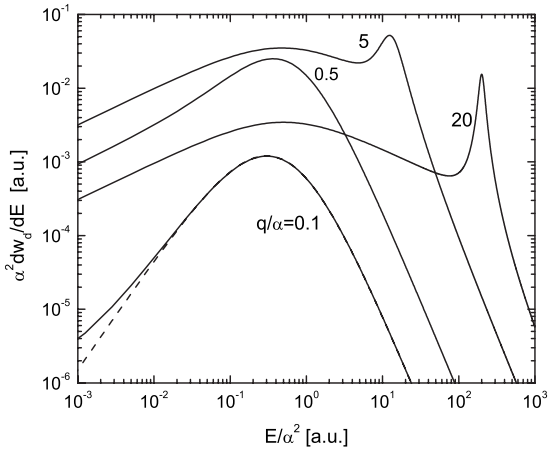

FIG. 3. Scaled energy distributions of detached electrons for indicated values of q/α in a.u. The dashed curve is the dipole-limit $(q\rightarrow 0)$ result from Eq. (18).

sented in Figs. 2(b) and 2(c). Also shown as dashed line, along with the curve corresponding to $q/\alpha=0.1$, is the dipole-limit $(q\rightarrow 0)$ result,

$$\frac{dw_d^d}{dE}=\frac{16\alpha q^2k^3}{3\pi(\alpha^2+k^2)^4}, \tag{18}$$

which follows from Eq. (16).

The angular distribution of the detached electrons is obtained by numerically integrating expression (15a) over k,

$$\frac{dw_d}{\sin\theta d\theta}=2\pi\int_0^\infty |a_{\mathbf{k}b}(\mathbf{q})|^2k^2dk. \tag{19}$$

The results for the four values of $q/\alpha=0.1$, 0.5, 5, and 20 are shown in Fig. 4. The dashed line is the dipole-limit $(q\rightarrow 0)$ result,

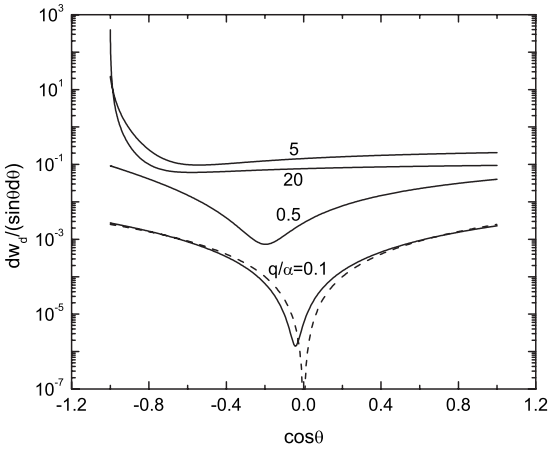

FIG. 4. Angular distributions of detached electrons for indicated values of q/α in a.u. The dashed curve is the dipole-limit $(q\rightarrow 0)$ result from Eq. (20).

$$\frac{dw_d^d}{\sin\theta d\theta}=\frac{q^2}{4\alpha^2}\cos^2\theta, \tag{20}$$

as obtained from Eq. (16). From Fig. 4 we see that as q/α increases, the angular distribution, which is symmetric in the dipole limit, becomes more and more peaked along the negative z axis $(\theta=\pi)$, in accord with Fig. 2.

We have verified that numerical integration of the distribution (17) over all energies and integration of the distribution (19) over all angles, both reproduce Fig. 1 and therefore confirm the formula (12).

III. TWO ALTERNATING ULTRASHORT HALF-CYCLE PULSES

We next consider the problem of electron detachment from a negative ion by two HCPs of the form (10), separated by a time interval τ. The case when both pulses have the same polarization and therefore transfer momentum to the electron in the same direction is not very interesting, since the second pulse simply "pushes" detached electron further away from the atom. Much more interesting is the case of two alternating pulses,

$$\tilde{\mathbf{F}}(t)=\mathbf{q}\delta(t)-\mathbf{q}\delta(t-\tau), \tag{21}$$

because the second pulse stops the propagation of the wave packet representing the electron detached after the first pulse and recapture of the electron can occur. In addition, we expect quantum interference effects produced by the wave packets originating from the first and the second pulses. Previously, the recapture was studied in the context of ionization of the hydrogen atom by HCPs [11,12]. The interference phenomena were studied in the context of the electron detachment from negative ions by using SFA [5] or numerical solutions [7], but for long pulses with durations satisfying the condition opposite to that given in Eq. (7).

The transition amplitude, in the case of the interaction with the two pulses (21), is given by

$$A_{fi}=\langle\psi_f|e^{i\mathbf{q}\cdot\mathbf{r}}e^{-iH_0\tau}e^{-i\mathbf{q}\cdot\mathbf{r}}|\psi_i\rangle. \tag{22}$$

In order to distinguish from the single-pulse case, the amplitudes and probabilities for the two-pulses case will be denoted by capital letters. Inserting now in Eq. (22) the complete set of ZRP eigenstates we obtain

$$A_{fi}=a_{fb}(-\mathbf{q})a_{bi}(\mathbf{q})e^{i(\alpha^2/2)\tau}+\int d^3\mathbf{p}a_{f\mathbf{p}}(-\mathbf{q})a_{\mathbf{p}i}(\mathbf{q})e^{-i(p^2/2)\tau}, \tag{23}$$

where the single-pulse amplitudes $a_{fi}(\mathbf{q})$ are defined in Eq. (8).

A. Total detachment probability

As in the case of a single pulse, the simplest to calculate from Eq. (23) is the amplitude of the probability for the electron to stay in the bound state,

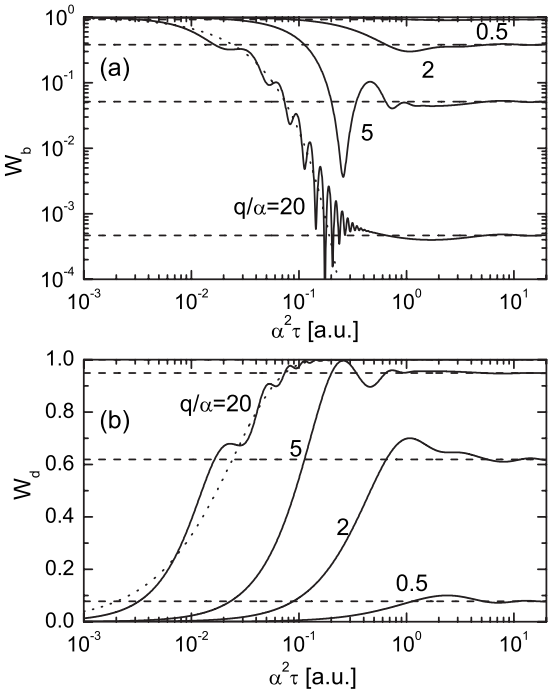

FIG. 5. (a) Probability of the electron to remain in the bound state W_b as a function of the scaled time interval $\alpha^2\tau$ between the pulses, for indicated values of q/α in a.u. The dashed lines are the large-τ asymptotes, Eq. (26). The dotted line is the large-q asymptote, Eq. (27), for $q/\alpha=20$. (b) Same as (a) but for the total detachment probability $W_d=1-W_b$.

$$A_{bb}=|a_{bb}(\mathbf{q})|^2e^{i(\alpha^2/2)\tau}+\int d^3\mathbf{p}|a_{\mathbf{p}b}(\mathbf{q})|^2e^{-i(p^2/2)\tau}, \quad (24)$$

where the single-pulse amplitudes $a_{bb}(\mathbf{q})$ and $a_{\mathbf{p}b}(\mathbf{q})$ are explicitly given in Eqs. (11) and (14).

The first term in Eq. (24) can be interpreted as the probability amplitude for the sequence of events in which the electron is not detached after the first pulse, evolves in the bound state of H_0 and is also not detached after the second pulse. The second term in Eq. (24) is the sum (integral) of the probability amplitudes which correspond to scenarios in which the electron is detached after the first pulse, evolves in the continuum of H_0 and is recaptured after the second pulse. These two terms coherently contribute to the total survival probability and we expect to see some quantum interference effects.

After performing angular integrations, the expression for the probability of the electron to remain in the bound state becomes

$$W_b=|A_{bb}|^2=\left|w_be^{i(\alpha^2/2)\tau}+\int_0^\infty\frac{dw_d}{dE}e^{-iE\tau}dE\right|^2, \quad (25)$$

where w_b and dw_d/dE are single-pulse survival probability and energy distribution of the detached electrons, given in Eqs. (12) and (17).

Figure 5(a) shows the survival probability (25) as a function of the scaled time interval $\alpha^2\tau$, for several values of q/α. For small values of $\alpha^2\tau$ this probability is close to 1. This is true even for large values of q/α where the detachment after the first pulse is very probable (see Fig. 1), indicating that the recapture of the electron after the second pulse is very efficient. Formally, this follows from the fact that the leading term of the expansion of W_b in Eq. (25) for $\alpha^2\tau, E_c(q)\tau\ll 1$ is $W_b\approx|w_b+w_d|^2=1$. Here, $E_c(q)$ is a cutoff value of energy for which the dw_d/dE is negligibly small (as seen from Fig. 3 this cutoff value is a function of q). In the opposite limit, for sufficiently large $\alpha^2\tau\gg 1$, the integral in Eq. (25) tends to zero and we have asymptotically,

$$W_b\asymp w_b^2. \quad (26)$$

This result simply indicates that for sufficiently large τ the recapture of the electron is negligible because the wave packet representing the detached electron after the first pulse is located very far away at the moment of action of the second pulse. The constant values from Eq. (26) are represented in Fig. 5(a) by horizontal dashed lines and they are indeed the asymptotes approached by the slowly oscillating W_b curves.

The case when $q\to\infty$ was studied in Ref. [17]. It was assumed that the initial state is completely depleted after the first pulse, i.e., $w_b=|a_{bb}(\mathbf{q})|^2\approx 0$. Retaining then in Eq. (24) only the integral and replacing the intermediate continuum states by plane waves, the following asymptotic expression was derived:

$$W_b\asymp e^{-2\alpha q\tau}. \quad (27)$$

This dependence is shown in Fig. 5(a) as a dotted line in the case $q/\alpha=20$. While the overall trend of W_b is well predicted, the oscillations are absent as they are due to the quantum interference which is not taken into account in Eq. (27). In addition, expression (27) is not valid for very long time intervals τ, because the constant term (26) then becomes dominant.

Figure 5(b) shows the total detachment probability $W_d=1-W_b$. It is just the mirror image of Fig. 5(a), but represented on the linear scale, so that the curve corresponding to $q/\alpha=0.5$ is now visible, while on the logarithmic scale of Fig. 5(a) it appears very close to $W_b=1$. In the special case of H^-, the interval from $\alpha^2\tau=0.01$ to $\alpha^2\tau=20$ corresponds to the range of $\tau=4.36$ as to $\tau=8.72$ fs.

Figure 6(a) shows the survival probability (25) as a function of q/α, for several values of the scaled time interval $\alpha^2\tau$. The dotted lines represent the large-q asymptotes, Eq. (27), and in the cases of $\alpha^2\tau=0.01$, 0.05, and 0.1 they (apart from the oscillations) indeed follow the general trend of the survival probabilities at large values of q/α. However, in the case of $\alpha^2\tau=0.5$, one can see that the corresponding dotted line is far from the exact result. The reason for this is that we have approached the large-τ asymptote, Eq. (26), represented by a dashed line in Fig. 6(a), where the expression (27) is no longer valid. Actually, the exact results for W_b, calculated for $\alpha^2\tau\geqslant 3$ are indistinguishable from the dashed line on the scale of Fig. 6(a).

The total detachment probability $W_d=1-W_b$ is shown in Fig. 6(b). Again, it is just the mirror image of Fig. 6(a) but represented on the linear scale.

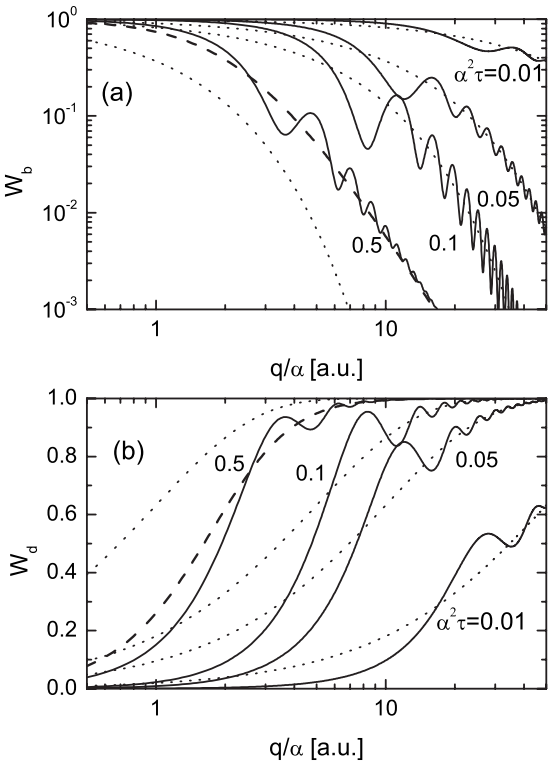

FIG. 6. (a) Probability of the electron to remain in the bound state W_b as a function of q/α, for indicated values of $\alpha^2\tau$ in a.u. The dotted lines are the large-q asymptotes, Eq. (27). The dashed line is the large-τ asymptote, Eq. (26). (b) Same as (a) but for the total detachment probability $W_d=1-W_b$.

B. Momentum, energy, and angular distributions

The detachment transition amplitude is obtained from Eq. (23),

$$A_{\mathbf{k}b} = a_{\mathbf{k}b}(-\mathbf{q})a_{bb}(\mathbf{q})e^{i(\alpha^2/2)\tau} + \int d^3\mathbf{p}\, a_{\mathbf{k}\mathbf{p}}(-\mathbf{q})a_{\mathbf{p}b}(\mathbf{q})e^{-i(p^2/2)\tau}, \tag{28}$$

where the bound-bound and bound-free single-pulse amplitudes $a_{bb}(\mathbf{q})$, $a_{\mathbf{p}b}(\mathbf{q})$, and $a_{\mathbf{k}b}(-\mathbf{q})$ are defined in Eqs. (11) and (14), whereas the free-free amplitude can be calculated from Eqs. (5) and (8) (see the Appendix),

$$\begin{aligned} a_{\mathbf{k}\mathbf{p}}(-\mathbf{q}) = \langle \psi_{\mathbf{k}}^{-}|e^{i\mathbf{q}\cdot\mathbf{r}}|\psi_{\mathbf{p}}^{-}\rangle = \delta(\mathbf{k}-\mathbf{q}-\mathbf{p}) \\ - \frac{1}{2\pi^2(\alpha-ip)(|\mathbf{k}-\mathbf{q}|^2-p^2+i\epsilon)} \\ - \frac{1}{2\pi^2(\alpha+ik)(|\mathbf{p}+\mathbf{q}|^2-k^2-i\epsilon)} \\ + \frac{1}{i4\pi^2 q(\alpha-ip)(\alpha+ik)} \ln\frac{i(p-k+q)+\epsilon}{i(p-k-q)+\epsilon}, \end{aligned} \tag{29}$$

where $\epsilon \to 0+$.

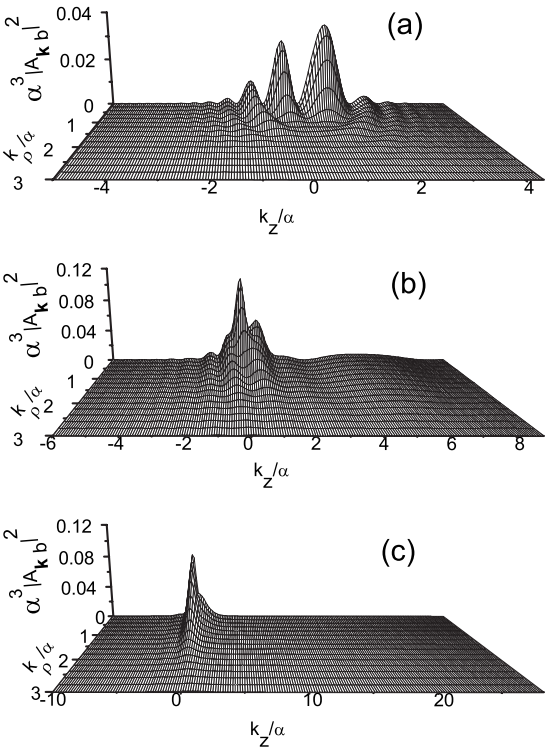

FIG. 7. Scaled momentum distributions of detached electrons for (a) $q/\alpha=0.5$, $\alpha^2\tau=5$, (b) $q/\alpha=5$, $\alpha^2\tau=1$, and (c) $q/\alpha=20$, $\alpha^2\tau=0.1$. All quantities are in a.u.

The first term in Eq. (28) can be interpreted as the probability amplitude for the sequence of events in which the electron is not detached after the first pulse, evolves in the bound state of H_0 and is detached after the second pulse. The second term in Eq. (24) is the sum (integral) of the probability amplitudes which correspond to scenarios in which the electron is detached after the first pulse, evolves in the continuum of H_0 and remains in the continuum after the second pulse. These two terms coherently contribute to the detachment probability and we also here expect to see some quantum interference effects.

Upon substitution of the expression (29), the calculation of the transition amplitude (28) can be reduced to evaluation of a single integral,

$$\begin{aligned} A_{\mathbf{k}b} = a_{\mathbf{k}b}(-\mathbf{q})a_{bb}(\mathbf{q})e^{i(\alpha^2/2)\tau} + a_{\mathbf{k}-\mathbf{q}b}(\mathbf{q})e^{-i[(|\mathbf{k}-\mathbf{q}|^2)/2]\tau} \\ - \frac{\alpha^{1/2}}{\pi^2}\int_0^\infty F(p;\mathbf{k},\mathbf{q})e^{-i(p^2/2)\tau}p^2dp, \end{aligned} \tag{30}$$

where the function $F(p;\mathbf{k},\mathbf{q})$ is explicitly given in the Appendix. The second term in Eq. (30) originates from the δ function in Eq. (29) and represents the contribution to detachment amplitude when the intermediate continuum states are approximated by plane waves. This term is dominant for large values of q, because as can be seen from explicit expressions in the Appendix, $F(p;\mathbf{k},\mathbf{q}) \to 0$ when $q \to \infty$.

Figure 7 shows the calculated momentum distributions for three characteristic pairs of parameters $(q/\alpha, \alpha^2\tau)$. In the $(q/\alpha, \alpha^2\tau)=(0.5,5)$ case [Fig. 7(a)], the interference pattern

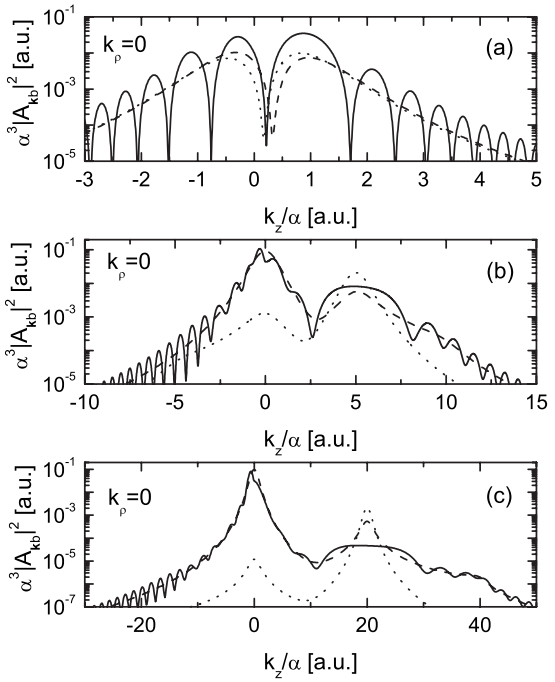

FIG. 8. Scaled momentum distributions of detached electrons at $k_\rho=0$ for (a) $q/\alpha=0.5$, $\alpha^2\tau=5$, (b) $q/\alpha=5$, $\alpha^2\tau=1$, and (c) $q/\alpha=20$, $\alpha^2\tau=0.1$. The dashed lines represent $\alpha^3|a_{\mathbf{k}-\mathbf{q}b}(\mathbf{q})|^2$ and the dotted lines represent $\alpha^3|a_{\mathbf{k}b}(-\mathbf{q})a_{bb}(\mathbf{q})|^2=\alpha^3 w_b|a_{\mathbf{k}b}(-\mathbf{q})|^2$.

is clearly visible. In the $(q/\alpha,\alpha^2\tau)=(5,1)$ case [Fig. 7(b)], the development of the peek at $\mathbf{k}=0$ is noticeable together with a wider structure around $k_z/\alpha=q/\alpha=5$. Finally, in the $(q/\alpha,\alpha^2\tau)=(20,0.1)$ case [Fig. 7(c)], the peak at the origin of the momentum space is the dominant feature.

Somewhat better understanding of the structures in the momentum distributions can be obtained from the analysis of the $k_\rho=0$ sections of these distributions, which are shown in Fig. 8 on the logarithmic scale. The dotted and dashed lines correspond, respectively, to the modulus squared of the first and second terms in Eq. (30). In the $(q/\alpha,\alpha^2\tau)=(0.5,5)$ case [Fig. 8(a)], we see that the interference pattern is predominant and actually, all three terms in Eq. (30) are more or less equally contributing. In the $(q/\alpha,\alpha^2\tau)=(5,1)$ case [Fig. 8(b)], the formation of the peek around $k_z=0$ is due to the second term in Eq. (30), while the broad structure around $k_z=q=5$ is the result of the interference of the first two terms. Finally, in the $(q/\alpha,\alpha^2\tau)=(20,0.1)$ case [Fig. 8(c)], the peak at $k_z=0$ is by far the predominant feature, while the interference structure around $k_z=q=20$ is still present but is orders of magnitude smaller [and therefore invisible on the linear scale of Fig. 7(c)].

The energy distribution of the detached electrons after the interaction with two alternating ultrashort pulses is given by

$$\frac{dW_d}{dE}=2\pi k\int_0^\pi |A_{\mathbf{k}b}|^2\sin\theta d\theta. \tag{31}$$

This quantity is shown in Fig. 9 for selected pairs of parameters $(q/\alpha,\alpha^2\tau)$. As compared to Fig. 8 the interference effects are less apparent, although for small q/α and large $\alpha^2\tau$ they become more pronounced.

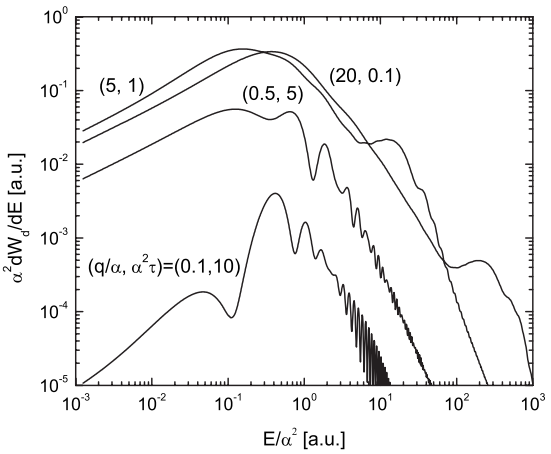

FIG. 9. Scaled energy distributions of detached electrons for indicated values of pairs of parameters $(q/\alpha,\alpha^2\tau)$ in a.u.

The angular distribution of the detached electrons is obtained as

$$\frac{dW_d}{\sin\theta d\theta}=2\pi\int_0^\infty |A_{\mathbf{k}b}|^2k^2dk. \tag{32}$$

Figure 10 shows the angular distributions for selected set of pairs of parameters $(q/\alpha,\alpha^2\tau)$. The interference effects are suppressed in these distributions.

We have verified that numerical integration of the energy distribution (31) over energies and integration of the angular distribution (32) over angles, both reproduce the total detachment probabilities calculated as $W_d=1-W_b$, with W_b given by Eq. (25). Thus, for the cases shown in Figs. 9 and 10, that is for the set of parameters $(q/\alpha,\alpha^2\tau)=(20,0.1)$, (5,1), (0.5,5), and (0.1,10) all three calculations give $W_d=0.97$, 0.95, 0.079, and 0.0033.

IV. CONCLUDING REMARKS

It should be noted that the unipolar HCPs are to a large extent theoretical idealizations. Actually, the closest to the

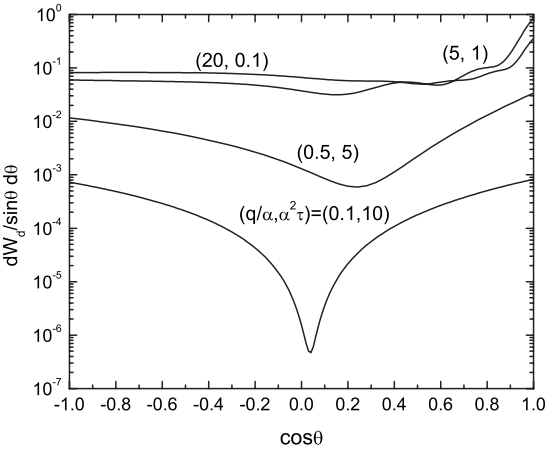

FIG. 10. Angular distributions of detached electrons for indicated values of pairs of parameters $(q/\alpha,\alpha^2\tau)$ in a.u.

"true HCPs" are the experimental pulses produced on a capacitor with the use of fast voltage pulse generators [18], with pulse durations of about 2 ns and used in studies of ionization of Rydberg atoms with $n \geqslant 300$. On the other hand, when freely propagating electromagnetic "HCPs" were used for studies of ionization of Rydberg atoms with $n = 15-35$ [19], they actually had a form of highly asymmetric single-cycle pulses, consisting of a short HCP (duration, ~0.5 ps) continuously followed by much longer HCP (duration, ~70 ps) of opposite polarity and much (about 10 times) smaller amplitude [20,21]. Additional investigations [22] have shown that the influence of the second HCP could be neglected (at least for considering the total ionization probabilities) only when its duration was much longer than the orbiting time of the Rydberg electron. The discussion of the actual form of the subfemptosecond HCPs, which are involved in the present study, will have to await their experimental realization.

In previous works [5,11,12] it has been pointed out that the analysis of the case of two oppositely polarized and time-delayed HCPs can help in describing the dynamics induced by a single-cycle pulse. The time delay τ must then be interpreted as one-half the period of the single-cycle pulse. Because, in this case, the first-order Magnus approximation is zero, the expression (22) is related to the second-order Magnus approximation [16]. There is a numerical evidence that in the case of ionization of the ground-state hydrogen atom (at least for survival probabilities at large momentum transfers) this is a good approximation [11,12]. In order to check if this also holds in the detachment problem one should confront our present results with the numerical solutions of the time-dependent Schrödinger equation in the case of a single-cycle pulse.

ACKNOWLEDGMENT

This work has been supported by the Ministry of Science and Technological Development of the Republic of Serbia through Contract No. 141029.

APPENDIX: EVALUATION OF INTEGRALS

The integrals that are used in analytical evaluations are the following ($\mathrm{Re}\,\lambda > 0$):

$$J(\lambda,\mathbf{q}) = \int e^{-\lambda r - i\mathbf{q}\cdot\mathbf{r}} \frac{d^3\mathbf{r}}{r^2} = \frac{2\pi}{iq} \ln\frac{\lambda + iq}{\lambda - iq}, \tag{A1}$$

$$I(\lambda,\mathbf{q}) = -\frac{\partial J}{\partial \lambda} = \int e^{-\lambda r - i\mathbf{q}\cdot\mathbf{r}} \frac{d^3\mathbf{r}}{r} = \frac{4\pi}{\lambda^2 + q^2}, \tag{A2}$$

$$K(\lambda,\mathbf{q}) = -\frac{\partial I}{\partial \lambda} = \int e^{-\lambda r - i\mathbf{q}\cdot\mathbf{r}} d^3\mathbf{r} = \frac{8\pi\lambda}{(\lambda^2 + q^2)^2}. \tag{A3}$$

The expressions for the single-pulse survival amplitude given by Eq. (11) and bound-free transition amplitude given by Eq. (14) rely on Eqs. (A1) and (A2). The formula (29) describing probability amplitude for the free-free transitions uses Eqs. (A1)–(A3) and the fact that for $\lambda \to 0+$, $K(\lambda,\mathbf{q}) \to (2\pi)^3 \delta(\mathbf{q})$.

The explicit expression for the function $F(p;\mathbf{k},\mathbf{q})$ introduced in Eq. (30) reads as

$$F(p;\mathbf{k},\mathbf{q}) = \frac{J_1(p,k) - f(p)J_2(p,k)}{\alpha + ik} + \frac{J_3(p) - 2f(p)}{\alpha - ip} \times \left(\frac{1}{|\mathbf{k}-\mathbf{q}|^2 - p^2 + i\epsilon} - g(p,k) \right), \tag{A4}$$

$$f(p) = \frac{1}{2iq(\alpha + ip)} \ln\frac{\alpha - i(p-q)}{\alpha - i(p+q)}, \tag{A5}$$

$$g(p,k) = \frac{1}{2iq(\alpha + ik)} \ln\frac{i(p-k+q) + \epsilon}{i(p-k-q) + \epsilon}, \tag{A6}$$

$$J_1(p,k) = \int_{-1}^{1} \frac{dx}{(p^2 + q^2 - k^2 + 2pqx - i\epsilon)(\alpha^2 + p^2 + q^2 + 2pqx)} = \frac{J_2(p,k) - J_3(p)}{\alpha^2 + k^2}, \tag{A7}$$

$$J_2(p,k) = \int_{-1}^{1} \frac{dx}{p^2 + q^2 - k^2 + 2pqx - i\epsilon} = \frac{1}{2pq} \ln\frac{(p+q)^2 - k^2 - i\epsilon}{(p-q)^2 - k^2 - i\epsilon}, \tag{A8}$$

$$J_3(p) = \int_{-1}^{1} \frac{dx}{\alpha^2 + p^2 + q^2 + 2pqx} = \frac{1}{2pq} \ln\frac{(p+q)^2 + \alpha^2}{(p-q)^2 + \alpha^2}. \tag{A9}$$

The existence of the term containing $i\epsilon$ in Eq. (A4) requires the use of the well-known formula

$$\int \frac{f(x)}{x - x_0 + i\epsilon} dx = \mathrm{P}\int \frac{f(x)}{x - x_0} dx - i\pi f(x_0) \tag{A10}$$

and numerical evaluation of the principal value (P) of the corresponding integral in Eq. (30).

The limit $\epsilon \to 0+$ also defines the proper phases of the arguments of the logarithms as being π for $k-q < p < k+q$ and zero otherwise in the case of Eq. (A6) and as being π for $|k-q| < p < k+q$ and zero otherwise in the case of Eq. (A8).

[1] Y. N. Demkov and V. N. Ostrovskii, *Zero-Range Potentials and Their Applications in Atomic Physics* (Plenum, New York, 1988).
[2] N. L. Manakov, M. V. Frolov, B. Borca, and A. F. Starace, J. Phys. B **36**, R49 (2003).
[3] P. Agostini and L. F. DiMauro, Rep. Prog. Phys. **67**, 813 (2004).
[4] G. Sansone, Science **314**, 443 (2006).
[5] S. X. Hu and A. F. Starace, Phys. Rev. A **68**, 043407 (2003).
[6] D. Dimitrovski and E. A. Solov'ev, J. Phys. B **39**, 895 (2006).
[7] C. Arendt, D. Dimitrovski, and J. S. Briggs, Phys. Rev. A **76**, 023423 (2007).
[8] C. O. Reinhold, M. Melles, H. Shao, and J. Burgdörfer, J. Phys. B **26**, L659 (1993).
[9] P. Krstić and Y. Hahn, Phys. Rev. A **50**, 4629 (1994).
[10] A. Bugacov, B. Piraux, M. Pont, and R. Shakeshaft, Phys. Rev. A **51**, 1490 (1995).
[11] D. Dimitrovski, E. A. Solov'ev, and J. S. Briggs, Phys. Rev. Lett. **93**, 083003 (2004).
[12] D. Dimitrovski, E. A. Solov'ev, and J. S. Briggs, Phys. Rev. A **72**, 043411 (2005).
[13] A. M. Dykhne and G. L. Yudin, Sov. Phys. Usp. **21**, 549 (1978).
[14] W. Magnus, Commun. Pure Appl. Math. **7**, 649 (1954).
[15] P. Pechukas and J. C. Light, J. Chem. Phys. **44**, 3897 (1966).
[16] M. Klaiber, D. Dimitrovski, and J. S. Briggs, J. Phys. B **41**, 175002 (2008).
[17] D. Dimitrovski, J. Poloczek, and J. S. Briggs, J. Phys. B **39**, 3019 (2006).
[18] C. O. Reinhold, J. Burgdörfer, M. T. Frey, and F. B. Dunning, Phys. Rev. A **54**, R33 (1996).
[19] R. R. Jones, D. You, and P. H. Bucksbaum, Phys. Rev. Lett. **70**, 1236 (1993).
[20] D. You, R. R. Jones, and P. H. Bucksbaum, Opt. Lett. **18**, 290 (1993).
[21] N. E. Tielking, T. J. Bensky, and R. R. Jones, Phys. Rev. A **51**, 3370 (1995).
[22] C. Wesdorp, F. Robicheaux, and L. D. Noordam, Phys. Rev. Lett. **87**, 083001 (2001).